Journal of Sound and Vibration (1997) **205**(2), 151–165

A TUNABLE TORSIONAL VIBRATION ABSORBER: THE CENTRIFUGAL DELAYED RESONATOR

M. Hosek, H. Elmali and N. Olgac

Department of Mechanical Engineering, University of Connecticut, Storrs, Connecticut, U.S.A.

(*Received* 28 *October* 1996, *and in final form* 17 *February* 1997)

A novel active vibration absorption device, the Centrifugal Delayed Resonator (CDR), is presented as an efficient way of eliminating undesired torsional oscillations in rotating mechanical structures. A damped centrifugal pendulum device is forced to mimic an ideal real-time tunable absorber utilizing a control torque in the form of proportional angular position feedback with variable gain and time delay. Strengths of the technique consist of total vibration suppression in the primary structure against harmonic torque excitation, full effectiveness of the absorber against time-varying frequency, very wide range of operating frequencies, complete decoupling of the feedback control from the structural and dynamic properties of the primary structure, extremely simple implementation of the control scheme, and fault-tolerant performance in the case of control failure.

1. INTRODUCTION

A great number of rotating mechanical structures (e.g., engine-driven electrical generator systems, crankshaft and transmission systems of aero, automobile and marine propulsion engines) are often loaded with cyclical forces that cause undesirable torsional oscillatory motions. Accepted ways of eliminating them are friction dampers and various dynamic absorber arrangements.

The *friction damper* [1–4] is an auxiliary device for dissipating energy by means of the frictional resistance between the primary structure* and a supplementary mass (Figure 1(a)). It is indiscriminate against the frequency of disturbance and, in general, less effective than comparable dynamic absorbers.

The *conventional torsional absorber* [3–6] is an auxiliary vibratory system that modifies the vibration characteristics of the primary structure. It consists of a supplementary mass elastically connected to the primary structure by a metallic or a rubber spring assembly (Figure 1(b)). The natural frequency of the spring controlled absorber is constant and the device is effective only when the frequency of disturbance coincides with the frequency to which it is tuned. Furthermore, when the conventional absorber is used to deal with a given resonant condition, its effect is to replace the troublesome resonant peak by two new resonant conditions, one below and the other above the original resonant peak.

This passive device fails to effectively treat cases where the frequency of disturbance varies in time. A recent active vibration absorption technique, the *delayed resonator* [7–9],

* Throughout the text, the following terms are used: the *primary structure* is the original rotating mechanical structure alone; *absorber unit* is the single vibration absorber assembly alone; and the *combined system* is the primary structure equipped with a set of absorber units.

0022–460X/97/320151 + 15 $25.00/0/sv970996

responds to this need. Using a control force in the form of the proportional position feedback with time delay, a conventional absorber setting is forced to mimic an ideal real-time tunable absorber (Figure 1(c)). Although the delayed resonator device completely removes undesired oscillations from the primary structure under the time-varying harmonic load, its applicability is limited to the cases where the frequency of disturbance fluctuates within a certain range around the natural frequency of the mass–spring–damper setting used. These limitations typically arise from stability and hardware related issues.

The *centrifugal pendulum absorber* [3, 4, 10, 11] is, again, an auxiliary vibratory arrangement in which the motion of the supplementary mass is controlled by a centrifugal force (Figure 1(d)). Since its natural frequency is directly proportional to the angular velocity of the primary structure, the centrifugal pendulum absorber can be adjusted to deal effectively even with a time-varying disturbance. However, the ratio of the frequency of disturbance and the angular velocity of the primary structure must remain constant.

In order to relax this requirement, a new active vibration elimination technique, the *centrifugal delayed resonator* (CDR), is proposed as a favorable synthesis of the centrifugal pendulum absorber and the delayed resonator control (Figure 2). Eliminating the frequency proportionality restriction of the centrifugal pendulum setting, it can respond to vibration problems with very wide frequency range. Typical examples can be seen in the crankshaft and transmission systems of aero, automobile and marine propulsion engines.

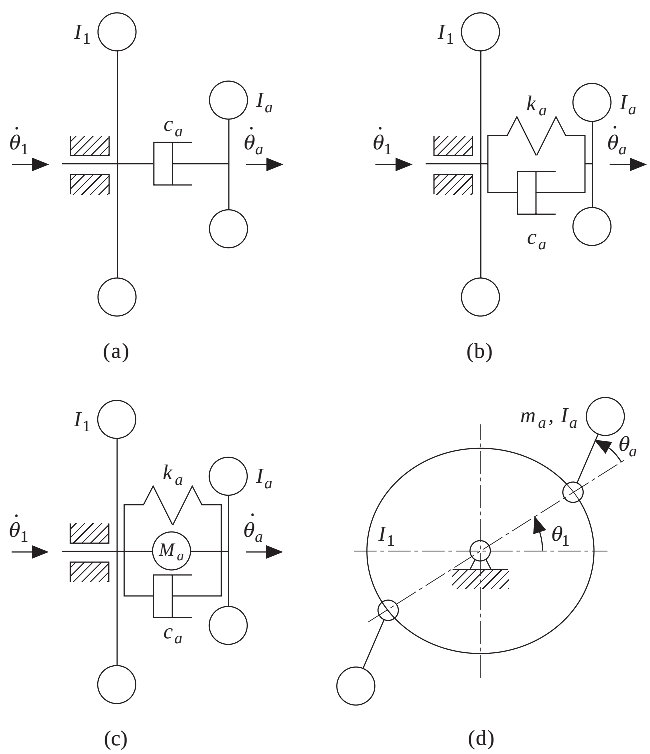

Figure 1. The friction damper (a), the conventional torsional absorber (b), the delayed resonator (c) and the centrifugal pendulum absorber (d). The following notation is used: I_1 and I_a denote the primary and absorber inertias, respectively, c_a and k_a represent the torsional damping and stiffness members, respectively, and M_a is a control torque in the form of the proportional position feedback with time delay; i.e., $M_a = g_c\theta_a(t - \tau_c)$.

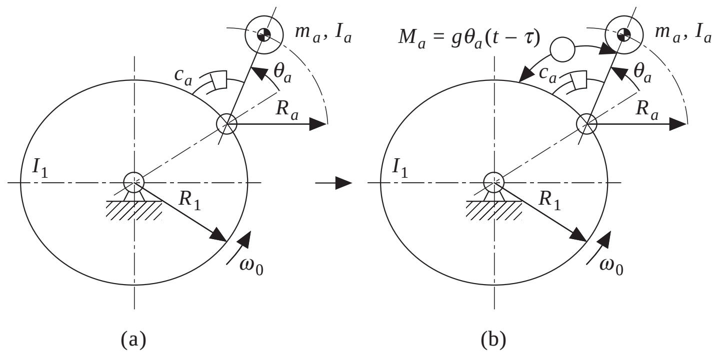

Figure 2. The damped centrifugal pendulum (a) and the centrifugal delayed resonator (b). $n_a = 1$; $\omega_0 =$ constant.

The CDR forms the core subject for this paper. Preliminary research results show rather exciting features which are sought after in industry.

2. THE CONCEPT OF THE CENTRIFUGAL DELAYED RESONATOR

The crucial idea in the CDR scheme is to reconfigure the dynamics of a damped centrifugal pendulum device such that it behaves like an ideal tunable resonator. Following the delayed resonator technique, the excitation torque M_a based on the proportional position feedback with a time delay is introduced to achieve this goal, as shown in Figure 2. For small displacements θ_a and constant angular velocity ω_0, the new system dynamics is represented by the linearized differential equation of motion

$$(I_a + m_a R_a^2)\ddot{\theta}_a(t) + c_a\dot{\theta}_a(t) + m_a R_1 R_a \omega_0^2 \theta_a(t) + g\theta_a(t-\tau) = 0. \tag{1}$$

The derivation of this equation is presented in Appendix A, in order not to disrupt the flow of the text. Also, a list of nomenclature is given in Appendix B. The corresponding Laplace domain representation leads to the transcendental characteristic equation

$$C(s) = (I_a + m_a R_a^2)s^2 + c_a s + m_a R_1 R_a \omega_0^2 + g\,\mathrm{e}^{-\tau s} = 0. \tag{2}$$

This equation possesses infinitely many roots. Their distribution for the gain g varying form zero to infinity while the time delay τ is constant can be studied from magnitude and angle conditions. Considering an underdamped centrifugal pendulum, the limiting cases are

$$\lim_{g\to 0} s = \begin{cases} -\dfrac{1}{2(I_a + m_a R_a^2)}\left[c_a \pm \sqrt{4(I_a + m_a R_a^2) m_a R_a R_i \omega_0^2 - c_a^2}\,\mathrm{i}\right], \\ -\infty \pm \dfrac{2l-1}{\tau}\pi\mathrm{i}, \qquad l = 1, 2, 3, \ldots, \end{cases} \tag{3}$$

$$\lim_{g\to\infty} s = +\infty \pm \frac{2l-1}{\tau}\pi\mathrm{i}, \qquad l = 1, 2, 3, \ldots. \tag{4}$$

With this information a typical root-locus plot can be sketched as shown in Figure 3, where the parameters $R_1 = 0{\cdot}15$ m, $R_a = 3{\cdot}749 \times 10^{-2}$ m, $I_a = 2 \times 10^{-7}$ kg m^2, $m_a = 0{\cdot}5$ kg, $c_a = 1{\cdot}406 \times 10^{-2}$ kg m^2/s, $\omega_0 = 500$ rad/s and $\tau = 1{\cdot}571 \times 10^{-3}$ s are used. To achieve the pure resonator behavior, two dominant roots of equation (2) should be placed on the imaginary axis at the desired resonant frequency, while other roots remain in the stable left-half plane. The proposition $s = \pm\omega_c\mathrm{i}$ as the solution of equation (2) yields

$$g_c = \sqrt{(c_a\omega_c)^2 + [(I_a + m_a R_a^2)\omega_c^2 - m_a R_1 R_a \omega_0^2]^2}, \tag{5}$$

$$\tau_c = \frac{a\tan 2[c_a\omega_c, (I_a + m_a R_a^2)\omega_c^2 - m_a R_1 R_a \omega_0^2] + 2(l_c - 1)\pi}{\omega_c}, \qquad l_c = 1, 2, 3.\ldots \tag{6}$$

The feedback gain g_c and delay τ_c are control parameters that can be set according to equations (5) and (6) to tune the CDR to the desired resonant frequency ω_c. This tuning can be done in real time. A set of solutions similar to equations (5) and (6) is also possible for negative values of the feedback gain g_c. However, for the sake of simplicity, it is kept outside the treatment of this text.

The implication of the parameter l_c can be visualized in plots of $g_c(\omega_c)$ versus $\tau_c(\omega_c)$ and ω_c versus τ_c, as depicted in Figures 4(a) and 4(b), respectively (the structural parameters remain the same as in Figure 3). For $l_c = 1$, i.e., the first branch of the root loci crosses the imaginary axis at the point of operation, there is a semi-infinite range of operating frequencies for a given angular velocity ω_0. The lower frequency bound ω_{A1} at the point A corresponds to the stability limit of the CDR as the second branch crosses to the unstable right half of the complex plane for the same gain and delay. For $l_c = 2$, i.e., the second branch of the root loci carrying the imaginary roots of interest, the range of operating frequencies is limited by both upper and lower bounds ω_{A2} and ω_{B1} due to the first and third branch crossings at the points A and B, respectively. It is easy to observe that for the frequency interval $\omega_{A2} > \omega_c > \omega_{B1}$, both the first and second branches (with different corresponding delays) can be used for the stable CDR operation.

Typical plots of the control parameters versus the resonant frequency, i.e., equations (5) and (6), are shown in Figures 5(a) and 5(b). The structural parameters R_a, I_a, m_a and c_a are selected in such a way that the natural frequency (and thus, approximately, the frequency of the resonant peak) of the lightly damped passive centrifugal pendulum assembly is twice the angular velocity of the rotating base (i.e., $\omega_a = 2\omega_0$; see Appendix A). Indeed, the example structure given above for Figures 3, 4 and 5 possesses this

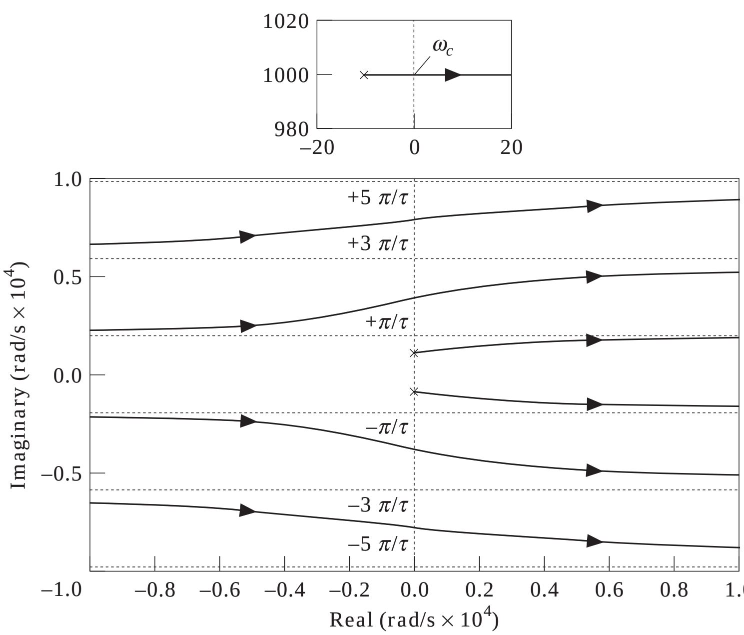

Figure 3. The root locus plot for the CDR. ×, Open-loop poles; —▶—, increasing g.

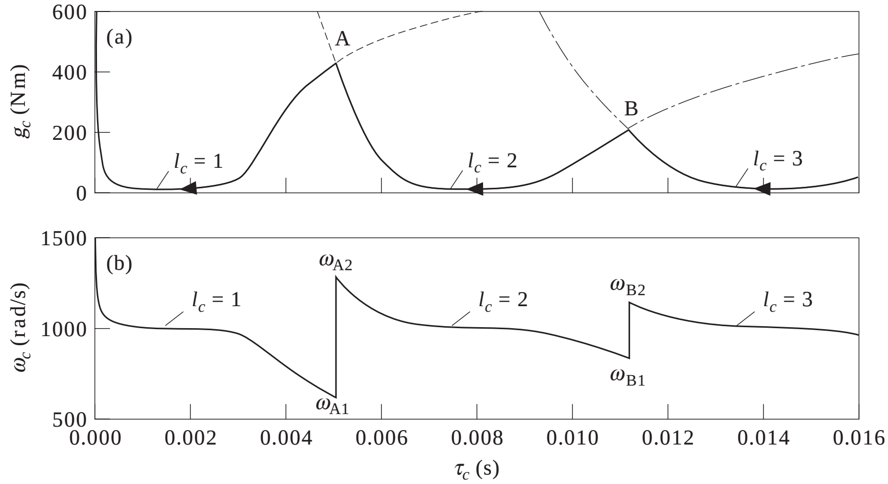

Figure 4. Plots of (a) $g_c(\omega_c)$ versus $\tau_c(\omega_c)$ and (b) ω_c versus τ_c. —▶—, increasing ω_c.

property. Solid curves represent graphs of $g_c(\omega_c)$ and $\tau_c(\omega_c)$ for different values of the angular velocity ω_0 in rad/s. Dashed curves correspond to the operating points for the order of resonant $n = 2$, where the order of resonance is defined as the ratio of the resonant frequency of the CDR and the angular velocity of the rotating base (i.e., $n = \omega_c/\omega_0$).

Compared to the delayed resonator based on the conventional mass–spring–damper setting [7–9], more relaxed limits of operating frequencies are expected to the advantage of the CDR device. These limitations typically arise from the stability and hardware related issues; for instance, when the required feedback gain g_c is too high or the sensitivity $S_{\tau_c,\omega_c} = \Delta\tau_c/\Delta\omega_c$ is very low.

The conventional delayed resonator can be represented by an equivalent angular velocity ω_0 in Figure 5, e.g., 500 rad/s for the natural frequency of 1000 rad/s. It is observed that the feedback gain g_c increases rapidly and that the sensitivity S_{τ_c,ω_c} decreases considerably

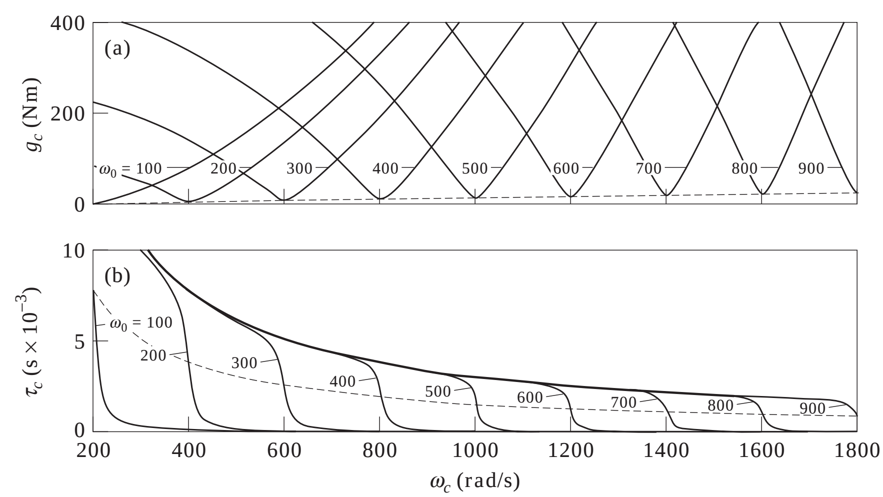

Figure 5. Control parameters versus the resonant frequency of the CDR, ω_0 (rad/s) parameter as marked.

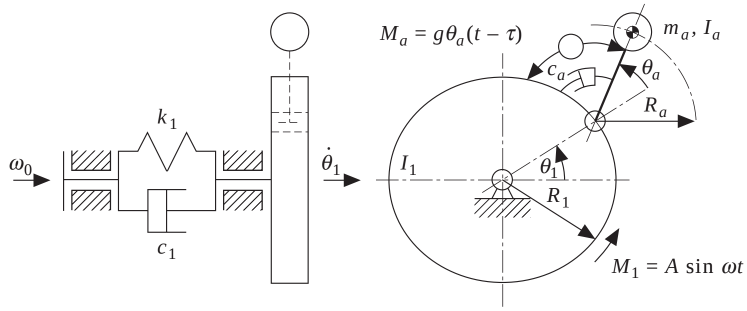

Figure 6. The SDOF system with the centrifugal delayed resonator. $n_a = 1$, $\omega_0 =$ constant.

when the resonant frequency ω_c departs from the neighborhood of the natural frequency of the mass–spring–damper setting used. That is, the tuning becomes more difficult to do.

On the other hand, as long as the frequency ω_c fluctuates around the order of resonance $n = 2$ (i.e., intersections of the solid and dashed lines in Figure 5), the CDR always operates near the minimum feedback gain g_c and the maximum sensitivity S_{τ_c,ω_c}. That means that the operation consumes relatively low energy and it is easy to tune. These features are very favorable when the CDR is used as a tuned dynamic absorber, as explained next.

3. THE CENTRIFUGAL DELAYED RESONATOR AS A VIBRATION ABSORBER

Attached to the primary structure disturbed by a harmonic load, the properly tuned CDR can act as an ideal torsional vibration absorber. The resulting combined system of the single-degree-of-freedom (SDOF) primary structure equipped with the CDR is depicted in Figure 6. For small displacements, the dynamics of the combined system are given by the following linearized system of simultaneous differential equations, as detailed in Appendix A:

$$[I_a + m_a(R_a^2 + R_1 R_a)]\ddot{\Delta}_1(t) + (I_a + m_a R_a^2)\ddot{\theta}_a(t) + c_a\dot{\theta}_a(t) + m_a R_1 R_a \omega_0^2 \theta_a(t) + g\theta_a(t-\tau) = 0, \quad (7)$$

$$[I_1 + n_a I_a + n_a m_a(R_1 + R_a)^2]\ddot{\Delta}_1(t) + C_1\dot{\Delta}_1(t) + K_1\Delta_1(t) + [n_a I_a + n_a m_a(R_a^2 + R_1 R_a)]\ddot{\theta}_a(t) - n_a c_a\dot{\theta}_a(t) - n_a g\theta_a(t-\tau) - M_1(t) = 0. \quad (8)$$

The corresponding Laplace domain representation leads to the following solution for the relative displacement of the primary structure:

$$\Delta_1(s) = \frac{C(s)}{A(s) + B(s)g\,\mathrm{e}^{-\tau s}} M(s). \quad (9)$$

The expressions $A(s)$ and $B(s)$ in the denominator are known polynomials of fourth and second order, respectively, and they are also defined in Appendix A. The numerator $C(s)$ is identical to the characteristic expression in equation (2). Therefore, as long as the denominator possesses stable roots and the CDR is tuned to the frequency of disturbance (i.e., $\omega = \omega_c$, $g = g_c$ and $\tau = \tau_c$), the primary structure exhibits no oscillatory motion in the steady state:

$$\lim_{t\to\infty} \Delta_1(t) = 0. \quad (10)$$

Equations (7) and (8) can be combined in the Laplace domain to obtain the transfer function between the disturbing torque M_1 and the absorber displacement θ_a. Setting $s = \pm\omega i$ and calculating the magnitude of the resulting expression yields the equation for the amplitude of the steady state oscillations of the absorber:

$$\max_{t\to\infty} \theta_a(t) = \frac{A}{n_a m_a R_a \omega^2\{2[I_a/(m_a R_a) + R_a] - [(\omega_0/\omega)^2 - 1]R_1\}}. \tag{11}$$

Based on equation (11), the absorber parameters I_a, m_a and n_a can be selected for the given amplitude of the disturbing torque A and the maximum absorber displacement θ_a allowed. This is an important design consideration, since the maximum absorber displacement is limited by the range of validity of the linear model given in equations (7) and (8).

Due to the linearity of the combined system, the frequency of excitation can be detected by observing the displacement of the absorber unit relative to the primary structure, as shown schematically in Figure 7. Since the control parameters are functions of the absorber structural parameters and the angular velocity of the rotating base only (see equations (5) and (6)), the CDR control scheme is entirely decoupled from the structural and dynamic parameters of the primary system.

Perfect vibration attenuation is achieved if the parameters involved in the expressions for g_c and τ_c (i.e., equations (5) and (6)) are known precisely. In many cases their values can only be estimated to a certain degree of accuracy and they may also change in time. In such applications an automatic tuning procedure is needed in order to robustize the CDR control against these uncertainties. A preliminary version of this procedure is described in reference [12]. The authors are mindful of the importance of this control robustization step; however, it is excluded from this text for the sake of brevity.

In summary, the properly tuned CDR can remove completely undesired vibrations from the primary structure under a harmonic torque disturbance. This property can be proven valid for a multi-degree-of-freedom (MDOF) primary structure as an extension to the development presented above.

4. STABILITY OF THE COMBINED SYSTEM

For the given angular velocity of the rotating base, the CDR absorber can effectively operate in a certain range of disturbing frequencies. While the upper bound of the range of operation typically arises from hardware related issues, the lower bound is dictated by

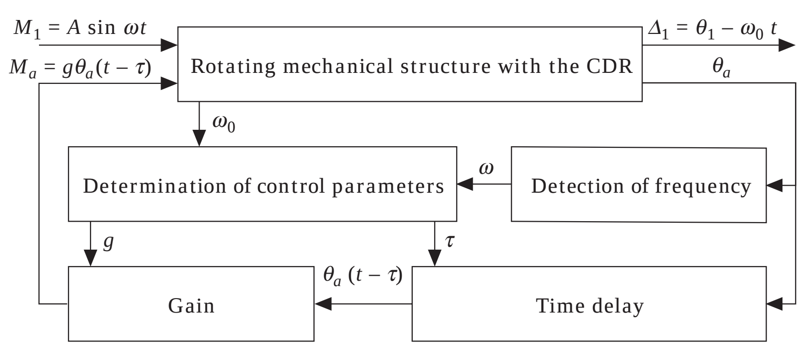

Figure 7. A block diagram of the CDR control scheme.

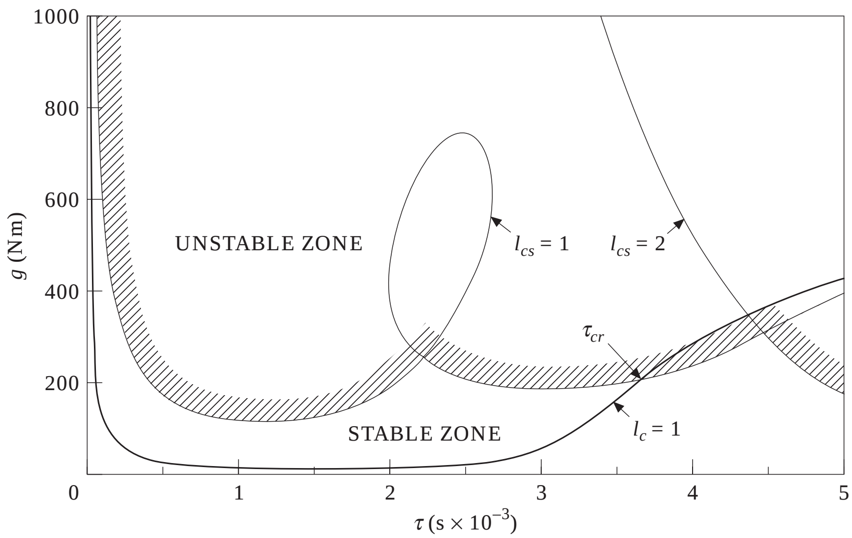

Figure 8. A gain–delay plot: the bold line represents $g_c(\omega_c)$ versus $\tau_c(\omega_c)$ and the light line $g_{cs}(\omega_{cs})$ versus $\tau_{cs}(\omega_{cs})$.

the stability limit of the combined system, as studied below. These operational limits can be found off-line during the design stage of the CDR.

The characteristic equation of the CDR alone (i.e., equation (2)) and the characteristic equation of the combined system*,

$$A(s) + B(s)g\ e^{-\tau s} = 0, \tag{12}$$

show a similar fundamental feature: linear dynamics with pure time delay. Therefore, the increasing feedback gain leading to instability of the combined system is expected. Consequently, the gain corresponding to the CDR operation should always remain smaller than the gain for which the combined system becomes unstable (for a given delay τ_c).

The feedback gain and delay which lead to the global system marginal stability are to be determined from its characteristic equation (12). At the point at which the root loci cross from the stable left half-plane to the unstable right half-plane, there are at least two roots of the characteristic equation on the imaginary axis; i.e., $s = \omega_{cs}\mathrm{i}$. Imposing this condition in equation (12) yields

$$g_{cs} = \left|\frac{A(\omega_{cs}\mathrm{i})}{B(\omega_{cs}\mathrm{i})}\right|, \quad \tau_{cs} = \frac{1}{\omega_{cs}}\left[(2l_{cs} - 1)\pi - \angle\frac{A(\omega_{cs}\mathrm{i})}{B(\omega_{cs}\mathrm{i})}\right], \qquad l_{cs} = 1, 2, 3, \ldots . \tag{13, 14}$$

As mentioned above, for a given τ_c the inequality of $g_c < g_{cs}$ should be satisfied for a stable operation. In order better to display this condition, it is convenient to study the corresponding zone of acceptable gains and delays in superposed parametric plots of $g_c(\omega_c)$ versus $\tau_c(\omega_c)$ for the CDR alone and $g_{cs}(\omega_{cs})$ versus $\tau_{cs}(\omega_{cs})$ for the combined system as depicted in Figure 8. For this particular figure the parameters of the primary structure are selected as $I_1 = 1{\cdot}125 \times 10^{-1}$ kg m^2, $c_1 = 22{\cdot}5$ kg m^2/s, $k_1 = 1{\cdot}125 \times 10^5$ kg m^2/s^2 and $R_1 = 0{\cdot}15$ m, the number of the absorber units is taken as $n_a = 2$, the absorber parameters are considered the same as in Figure 3 and the angular velocity of the base remains

* The expressions $A(s)$ and $B(s)$ in equation (12) are polynomials of fourth and second order, respectively, defined by equations (A21)–(A27) in Appendix A.

$\omega_0 = 500$ rad/s. Implementing the condition expressed above, i.e., $g_c < g_{cs}$, an operable range is found as $\tau < \tau_{cr}$ with the critical time delay $\tau_{cr} = 3{\cdot}646 \times 10^{-3}$ s. The corresponding frequency range is $\omega_c > \omega_{cr}$, with the lower bound $\omega_{cr} = 845{\cdot}5$ rad/s.

Repeating the same stability analysis for a varying angular velocity ω_0 in a given range of interest, the stability diagram can be generated as shown in Figure 9. These critical frequencies can be built into the control algorithm to assure operation of the CDR only in the stable range. That is, at a given ω_0, any disturbance $\omega \leqslant \omega_{cr}$ must be identified as *inoperable*. As a preferred alternative, this scheme can be utilized to design the CDR absorber in such a way that the expected frequencies of disturbance remain *operable*.

The combined system is subject to changes in two parameters which can possibly jeopardize its stability: the angular velocity ω_0 and the frequency of disturbance ω. Any change in the angular velocity ω_0 has a direct influence on the stability properties of the combined system. In reality, however, the changes are smooth and comparably slow due to the inertias involved in the rotating structure. Since ω_0 is monitored continuously for the CDR tuning (see equations (5) and (6)), the stability limits ω_{cr} can be updated periodically based on these measurements. The frequency of disturbance ω, on the other hand, is a property of the external disturbance. Therefore, it has no influence on the system stability until the control parameters g_c and τ_c are modified to correspond to the detected value of ω. Naturally, the controller should decide on these modifications only if the condition of $\omega > \omega_{cr}$ is satisfied.

In summary, the following steps are taken at every instant when ω_0 or ω is updated: (a) the stability limit ω_{cr} is determined; (b) the frequency of disturbance ω is compared with the current stability limit ω_{cr}; (c) for $\omega > \omega_{cr}$, the control parameters should be implemented according to equations (5) and (6); (d) for $\omega \leqslant \omega_{cr}$, the passive mode should be introduced by setting $g = 0$. The last case, however, should be prevented by proper design of the CDR for expected operating frequencies, as mentioned earlier.

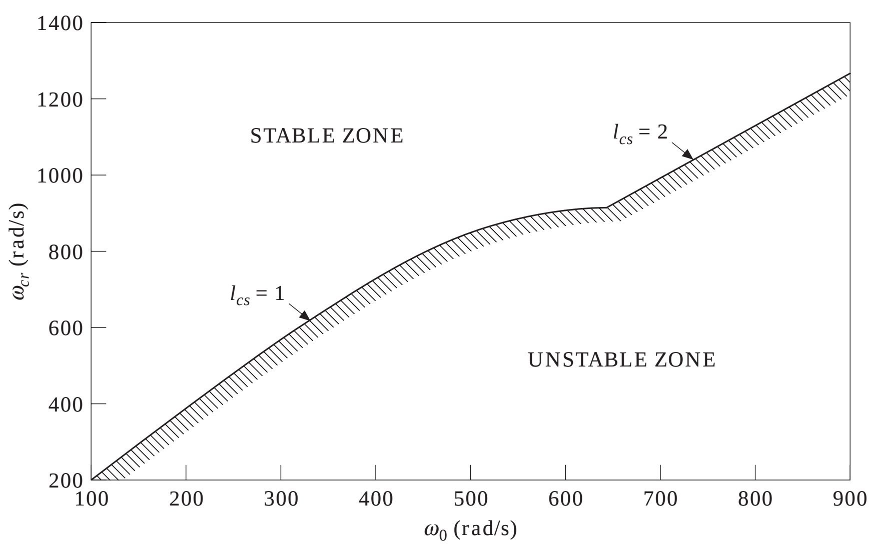

Figure 9. The stability diagram for the combined system.

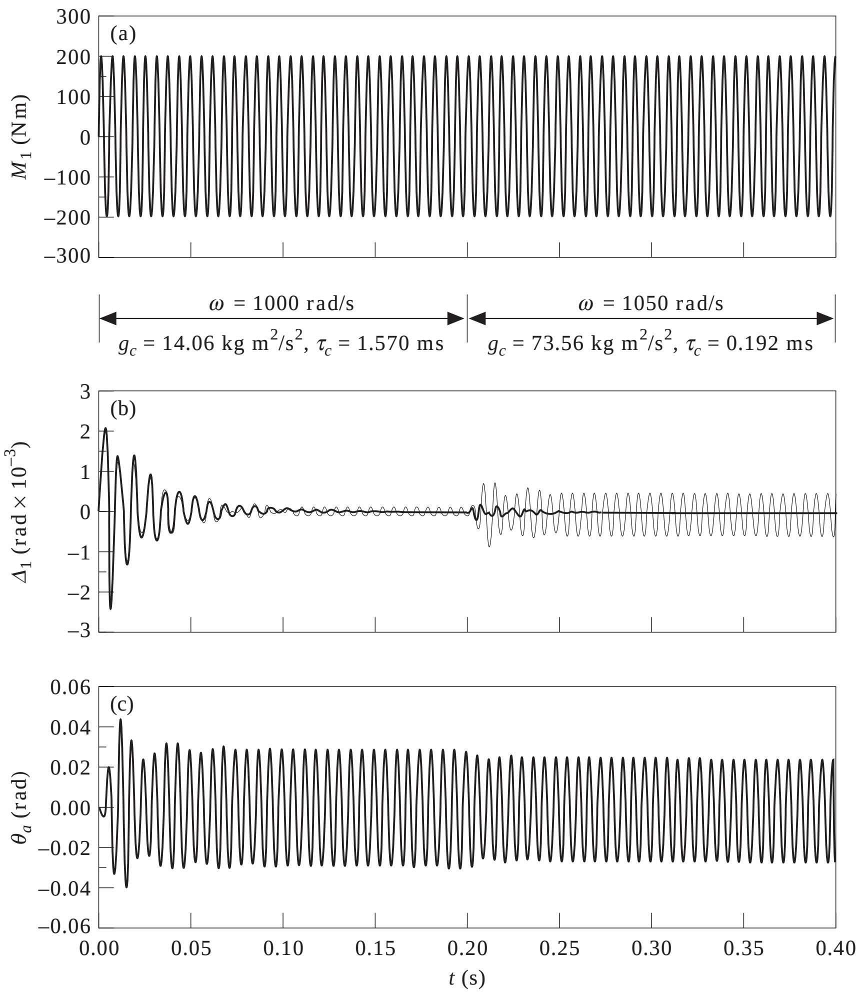

Figure 10. The simulated time response of the combined system: (a) the disturbance torque; (b) the relative displacement of the primary structure (the bold line is for the CDR and the light line for a passive centrifugal pendulum absorber); (c) the angular displacement of the CDR absorber.

5. SIMULATION EXAMPLE

The characteristics claimed above can be verified by the time response simulation of an example combined system. The primary structure is taken as a cylindrical body with a mass of 10 kg, a radius of 0·15 m, a natural frequency of 1000 rad/s and a damping ratio of 0·1, which leads to the structural parameters $I_1 = 1{\cdot}125 \times 10^{-1}$ kg m^2, $c_1 = 22{\cdot}5$ kg m^2/s, $k_1 = 1{\cdot}125 \times 10^5$ kg m^2/s^2 and $R_1 = 0{\cdot}15$ m. The frequency of disturbance is assumed to fluctuate within a certain interval around the order of disturbance $n = 2$. Therefore, the CDR assembly is designed in such a way that the resonant peak of the uncontrolled absorber matches $2\omega_0$ (see Appendix A). If the damping ratio of the absorber unit is taken as 0·01, the corresponding structural parameters are $I_a = 2 \times 10^{-7}$ kg m^2, $m_a = 0{\cdot}5$ kg, $c_a = 1{\cdot}406 \times 10^{-2}$ kg m^2/s and $R_a = 3{\cdot}749 \times 10^{-2}$ m. The number of absorber units attached to the primary structure is selected as $n_a = 2$.

The time response simulation using the non-linear model of the combined system (as given in Appendix A) is represented by the bold line in Figure 10. The primary structure rotating at the constant angular velocity $\omega_0 = 500$ rad/s is disturbed by the harmonic torque M_1 of amplitude $A = 200$ Nm and frequency $\omega = 1000$ rad/s. It can be observed that, after approximately 0·12 s of transient response, all undesired oscillations are practically removed from the primary structure. That is, a negating torque is implemented by the CDR on the primary structure to eliminate the effect of the harmonic disturbance. At $t = 0{\cdot}2$ s a step change in the disturbance frequency takes place from 1000 rad/s to 1050 rad/s. After another transient period of approximately the same duration, the vibration suppression of the primary structure takes place and the absorber settles at a new steady state amplitude.

The light line in Figure 10(b) represents the behavior of the system with a damped centrifugal pendulum absorber (i.e., no control feedback is used). The vibration suppression is acceptable only in the first half of the test (i.e., for $t < 0{\cdot}2$ s). This is expected because the centrifugal pendulum is tuned to show a peak response at 1000 rad/s. The effect of the damping, however, is noticeable in the form of non-zero residual oscillations in the primary structure. It is seen that in the case of control failure the CDR can turn itself into a passive absorber with a partial effectiveness, which can be considered the fail-tolerant feature of the CDR method.

6. CONCLUSIONS

The centrifugal delayed resonator is presented as a tunable device for active suppression of torsional vibrations in rotating mechanical structures. Its attractive features over the vibration control techniques in current practice can be summarized as follows:

(1) In steady state, the CDR is capable to completely eliminate undesired oscillations of the primary structure under a harmonic torque disturbance.

(2) Due to its real-time tuning, the CDR is fully effective for vibration problems with a time-varying harmonic disturbance. It can deal with an extremely wide frequency range, especially in cases in which the frequency of disturbance tends to increase with the angular velocity of the primary structure.

(3) The control scheme is decoupled from the structural and dynamic properties of the primary structure to which the CDR is attached.

(4) The control algorithm for the CDR is simple to implement, especially utilizing advanced digital signal processing devices.

(5) Due to its hybrid (i.e., active–passive) character, the CDR can still be partially effective even in the case of control failure, assuming that the passive centrifugal pendulum absorber used is tuned properly.

ACKNOWLEDGMENTS

The work presented is supported in part by a grant from the National Science Foundation (grant no. CMS-9415428) and by the Variable Frequency Vibration Elimination Consortium at the University of Connecticut (with active members Pratt & Whitney of United Technologies and Electric Boat of General Dynamics).

REFERENCES

1. F. W. Lanchester 1910 *British Patent* 21,139. Improvements relating to high speed reciprocating engines.
2. J. P. Den Hartog and J. Ormondroyd 1930 *Transactions of the American Society of Mechanical Engineers* **52**, 133. Torsional vibration dampers.

3. W. K. WILSON 1968 *Practical Solution of Torsional Vibration Problems*. London: Chapman & Hall.
4. W. T. THOMSON 1988 *Theory of Vibration with Applications*. Englewood Cliffs, New Jersey: Prentice-Hall.
5. H. FRAHM 1911 *United States Patent* 989,958. Device for damping vibrations of bodies.
6. J. ORMONDROYD and J. P. DEN HARTOG 1928 *Transactions of the American Society of Mechanical Engineers* **50**, 9–22. The theory of the dynamic vibration absorber.
7. N. OLGAC and B. HOLM-HANSEN 1995 *Transactions of the American Society of Mechanical Engineers*, *Journal of Dynamic Systems*, *Measurement and Control* **117**, 513–519. Tunable active vibration absorber: the delayed resonator.
8. N. OLGAC 1995 *United States Patent* 5,431,261. Delayed resonators as active dynamic absorbers.
9. N. OLGAC and M. HOSEK 1997 *Transactions of the American Society of Mechanical Engineers*, *Journal of Vibration and Acoustics* **119**, 131–136. Active vibration absorption using delayed resonator with relative position measurement.
10. B. C. CARTER 1929 *British Patent* 337,466. Improvements in or relating to damping or oscillation-checking devices.
11. J. P. DEN HARTOG 1938 *Stephen Timoshenko 60th Anniversary Volume*, *Tuned Pendulums as Torsional Vibration Eliminators*. London: Macmillan.
12. M. E. RENZULLI 1996 *M.S. Thesis*, *University of Connecticut*. An algorithm for automatic tuning of the delayed resonator vibration absorber.

APPENDIX A: DERIVATIONS

A.1. NON-LINEAR EQUATIONS OF MOTION

The mechanical structure under consideration (the combined system) is shown in Figure 6. The base rotating with the constant angular velocity ω_0 carries the SDOF primary structure (with parameters R_1, I_1, c_1 and k_1) which is acted on by the disturbing torque M_1. The primary structure is equipped with n_a absorber units (with parameter R_a, I_a, m_a and c_a), each of which is controlled by the torque M_a based on the proportional position feedback with time delay.

The velocity of the typical absorber unit attached to the rotating primary structure is given by the expression

$$v_a^2 = R_1^2\dot{\theta}_1^2 + R_a^2(\dot{\theta}_1 + \dot{\theta}_a)^2 + 2R_1R_a(\dot{\theta}_1^2 + \dot{\theta}_1\dot{\theta}_a)\cos\theta_a. \tag{A1}$$

The kinetic energy composed of the translational and rotational components of the absorber unit motion is

$$E_a = \tfrac{1}{2}\{I_a(\dot{\theta}_1 + \dot{\theta}_a)^2 + m_a[R_1^2\dot{\theta}_1^2 + R_a^2(\dot{\theta}_1 + \dot{\theta}_a)^2 + 2R_1R_a(\dot{\theta}_1^2 + \dot{\theta}_1\dot{\theta}_a)\cos\theta_a]\}. \tag{A2}$$

The kinetic energy of the rotational motion of the primary structure can be expressed simply as

$$E_1 = \tfrac{1}{2}I_1\dot{\theta}_1^2. \tag{A3}$$

Assuming that the influence of gravity forces is negligible, the Lagrangian function has the form

$$L = \tfrac{1}{2}\{I_1\dot{\theta}_1^2 + n_aI_a(\dot{\theta}_1 + \dot{\theta}_a)^2 + n_am_a[R_1^2\dot{\theta}_1^2 + R_a^2(\dot{\theta}_1 + \dot{\theta}_a)^2 + 2R_1R_a(\dot{\theta}_1^2 + \dot{\theta}_1\dot{\theta}_a)\cos\theta_a]\}. \tag{A4}$$

Taking the angular displacements θ_1 and θ_a as generalized co-ordinates, the corresponding generalized forces are

$$Q_1 = -C_1(\dot{\theta}_1 - \omega_0) - K_1(\theta_1 - \omega_0 t) + n_ac_a\dot{\theta}_a + n_ag\theta_a(t-\tau) + M_1, \tag{A5}$$

$$Q_a = -n_ac_a\dot{\theta}_a - n_ag\theta_a(t-\tau). \tag{A6}$$

With this information, the Lagrange's equations of motion for the combined system can be written as

$$Q_1 = \frac{\mathrm{d}}{\mathrm{d}t}\left(\frac{\partial L}{\partial \dot{\theta}_1}\right) - \frac{\partial L}{\partial \theta_1}, \qquad Q_a = \frac{\mathrm{d}}{\mathrm{d}t}\left(\frac{\partial L}{\partial \dot{\theta}_a}\right) - \frac{\partial L}{\partial \theta_a}. \tag{A7, A8}$$

Differentiating L and introducing the relative displacement of the primary structure, $\Delta_1 = \theta_1 - \omega_0 t$, yields the following system of simultaneous non-linear differential equations of motion:

$$\begin{aligned}&[I_1 + n_a I_a + n_a m_a(R_1^2 + R_a^2 + 2R_1 R_a \cos\theta_a)]\ddot{\Delta}_1 + [n_a I_a + n_a m_a(R_a^2 + R_1 R_a \cos\theta_a)]\ddot{\theta}_a \\ &\quad - n_a m_a R_1 R_a[2(\omega_0 + \dot{\Delta}_1)\dot{\theta}_a + \dot{\theta}_a^2]\sin\theta_a - C_1\dot{\Delta}_1 + K_1\Delta_1 - n_a c_a\dot{\theta}_a - n_a g\theta_a(t-\tau) - M_1 = 0,\end{aligned} \tag{A9}$$

$$\begin{aligned}&[I_a + m_a(R_a^2 + R_1 R_a\cos\theta_a)]\ddot{\Delta}_1 + (I_a + m_a R_a^2)\ddot{\theta}_a \\ &\quad + m_a R_1 R_a(\omega_0 + \dot{\Delta})^2 \sin\theta_a + c_a\dot{\theta}_a + g\theta_a(t-\tau) = 0.\end{aligned} \tag{A10}$$

A.2. LINEARIZED EQUATIONS OF MOTION

Assuming small angular displacements, the non-linear equations of motions can be linearized in the neighborhood of the point of stable equilibrium (i.e., $M_1 = 0$, $\Delta_1 = \dot{\Delta}_1 = \ddot{\Delta}_1 = 0$ and $\theta_a = \dot{\theta}_a = \ddot{\theta}_a = 0$). As a favorable result, the theory of linear systems can be used to study the dynamic properties of the combined system and its components.

A.2.1. *Combined system*

Denoting the left sides in equations (A9) and (A10) by f_1 and f_a, respectively, the equations of motion can be linearized in the neighborhood of the point of equilibrium O as

$$\begin{aligned}&[\partial f_1/\partial\ddot{\Delta}_1]_0\ddot{\Delta}_1 + [\partial f_1/\partial\dot{\Delta}_1]_0\dot{\Delta}_1 + [\partial f_1/\partial\Delta_1]_0\Delta_1 + [\partial f_1/\partial\ddot{\theta}_a]_0\ddot{\theta}_a + [\partial f_1/\partial\dot{\theta}_a]_0\dot{\theta}_a \\ &\quad + [\partial f_1/\partial\theta_a]_0\theta_a + [\partial f_1/\partial\theta_a(t-\tau)]_0\theta_a(t-\tau) + [\partial f_1/\partial M_1]_0 M_1 = 0,\end{aligned} \tag{A11}$$

$$\begin{aligned}&[\partial f_a/\partial\ddot{\Delta}_1]_0\ddot{\Delta}_1 + [\partial f_a/\partial\dot{\Delta}_1]_0\dot{\Delta}_1 + [\partial f_a/\partial\ddot{\theta}_a]_0\ddot{\theta}_a \\ &\quad + [\partial f_a/\partial\dot{\theta}_a]_0\dot{\theta}_a + [\partial f_a/\partial\theta_a]_0\theta_a + [\partial f_a/\partial\theta_a(t-\tau)]_0\theta_a(t-\tau) = 0.\end{aligned} \tag{A12}$$

Evaluating the partial derivatives involved, yields the following system of simultaneous transcendental differential equations of motion for the combined system:

$$\begin{aligned}&[I_1 + n_a I_a + n_a m_a(R_1 + R_a)^2]\ddot{\Delta}_1 + C_1\dot{\Delta}_1 + K_1\Delta_1 \\ &\quad + [n_a I_a + n_a m_a(R_a^2 + R_1 R_a)]\ddot{\theta}_a - n_a c_a\dot{\theta}_a - n_a g\theta_a(t-\tau) - M_1 = 0,\end{aligned} \tag{A13}$$

$$[I_a + m_a(R_a^2 + R_1 R_a)]\ddot{\Delta}_1 + (I_a + m_a R_a^2)\ddot{\theta}_a + c_a\dot{\theta}_a + m_a R_1 R_a\omega_0^2\theta_a + g\theta_a(t-\tau) = 0. \tag{A14}$$

A.2.2. *Centrifugal delayed resonator*

To study the dynamics of the CDR alone, the primary structure is assumed to be rigidly connected to the rotating base; that is, $\Delta_1 = \dot{\Delta}_1 = \ddot{\Delta}_1 = 0$. With this proposition, equation (A14) takes the form

$$(I_a + m_a R_a^2)\ddot{\theta}_a + c_a\dot{\theta}_a + m_a R_1 R_a\omega_0^2\theta_a + g\theta_a(t-\tau) = 0. \tag{A15}$$

A.2.3. *Uncontrolled absorber unit*

At the stage of the CDR design (i.e., proper selection of the structural parameters R_a, I_a, m_a and c_a), the dynamics of the uncontrolled absorber unit should be analyzed. Replacing $g\theta_a(t-\tau)$ by M_a in equation (A15) yields the equation of motion for forced oscillations of the damped centrifugal pendulum absorber alone:

$$(I_a + m_a R_a^2)\ddot{\theta}_a + c_a\dot{\theta} + m_a R_1 R_a \omega_0^2 \theta_a = M_a. \tag{A16}$$

The relationships between the structural parameters and the corresponding natural frequency and damping ratio become

$$\omega_a = \sqrt{\frac{R_1}{R_a + I_a/(m_a R_a)}}\,\omega_0, \qquad \zeta_a = \frac{c_a}{2\omega_0\sqrt{m_a R_1 R_a (I_a + m_a R_a^2)}}. \tag{A17, A18}$$

The resonant peak of the frequency response of the uncontrolled absorber occurs at the frequency of excitation (for light damping)

$$\omega_p = \omega_a\sqrt{1 - 2\zeta_a^2} \approx \omega_a. \tag{A19}$$

A.3. CHARACTERISTIC EQUATION

Based on the Laplace representation of equations (7) and (8), the characteristic equation of the combined system can be written as

$$A(s) + B(s)g\,\mathrm{e}^{-\tau s} = 0. \tag{A20}$$

The expressions $A(s)$ and $B(s)$ are polynomials of fourth and second order, respectively, defined as

$$A(s) = a_4 s^4 + a_3 s^3 + a_2 s^2 + a_1 s + a_0, \qquad a_0 = m_a k_1 R_1 R_a \omega_0^2,$$

$$a_1 = m_a c_1 R_1 R_a \omega_0^2 + c_a k_1, \tag{A21–A23}$$

$$a_2 = k_1(I_a + m_a R_a^2) + m_a R_1 R_a \omega_0^2[I_1 + n_a I_a + n_a m_a (R_1 + R_a)^2] + c_1 c_a, \tag{A24}$$

$$a_3 = I_1 c_a + I_a(2n_a c_a + c_1) + m_a[c_1 R_a^2 + n_a c_a(R_1^2 + 2R_a^2 + 3R_1 R_a)], \tag{A25}$$

$$a_4 = I_1 I_a + m_a(n_a I_a R_1^2 + I_1 R_a^2), \tag{A26}$$

$$B(s) = \{I_1 + n_a[2I_a + m_a(R_1^2 + 2R_a^2 + 3R_1 R_a)]\}s^2 + c_1 s + k_1. \tag{A27}$$

APPENDIX B: NOMENCLATURE

A	amplitude of the disturbing torque acting on the primary structure (Nm)
c_a	damping coefficient of the absorber unit (kg m^2/s)
c_1	damping coefficient of the primary structure (kg m^2/s)
E_a	kinetic energy of the absorber unit (J)
E_1	kinetic energy of the primary structure (J)
g	control feedback gain (Nm)
I_a	inertia moment of the absorber unit about the center of mass (kg m^2)
I_1	inertia moment of the primary structure about the center of rotation (kg m^2)
k_1	stiffness coefficient of the primary structure (kg m^2/s^2)
L	Lagrangian function (J)
M_1	disturbing torque acting on the primary structure (Nm)
M_a	control torque acting on the absorber unit (Nm)
m_a	mass of the absorber unit (kg)
n	order of disturbance (–)
n_a	number of absorber units attached to the primary structure (–)

R_a distance between the point of suspension of the absorber unit and the center of mass of the absorber unit (m)
R_1 distance between the center of rotation of the primary structure and the point of suspension of the absorber unit (m)
S_{τ_c,ω_c} sensitivity of τ_c with respect to ω_c (m/s)
v_a translational velocity of the center of mass of the absorber unit (s^2/rad)
Δ_1 angular displacement of the primary structure relative to the rotating base (rad)
ζ_a damping ratio of the absorber unit (−)
θ_a angular displacement of the absorber unit relative to the primary structure (rad)
θ_1 angular displacement of the primary structure relative to the fixed frame of reference (rad)
τ control feedback delay (s)
τ_{cr} critical feedback delay (s)
ω frequency of the disturbing torque acting on the primary structure (rad/s)
ω_a natural frequency of the passive absorber unit (rad/s)
ω_c resonant frequency of the centrifugal delayed resonator (rad/s)
ω_{cr} critical frequency of operation (rad/s)
ω_{cs} resonant frequency of the combined system (rad/s)
ω_0 angular velocity of the rotating base (rad/s)
ω_p peaking frequency of the passive absorber unit (rad/s)